

2020 年臺灣國際科學展覽會 優勝作品專輯

作品編號 090027
參展科別 醫學與健康科學
作品名稱 Lighting Up The Brain
得獎獎項 大會獎：一等獎
青少年科學獎

國家 Canada
就讀學校 Dawson College
作者姓名 Shaan Baig

關鍵詞 Alzheimer's disease,
Carbon dot(CD)-bound bispecific antibody,
fNIR- spectroscopy

作者照片



Abstract: Alzheimer's disease (AD) is a neurodegenerative disease in which current diagnostic tools are invasive and lack the ability to diagnose early-onset dementia. Current antibody-based diagnostic tests for neurodegenerative diseases require invasive measures such as a lumbar puncture, and lack specificity to biomarkers that are found in both healthy individuals and patients with AD. In this project, a design for a carbon dot(CD)-bound bispecific antibody is developed for the minimally-invasive diagnosis of AD. The molecular probe can be easily synthesized with a specificity to amyloid-beta ($A\beta$) oligomers as its distribution and abundance in the brain suggest they are better predictors of disease progression and are present in the early-onset of the dementia. The bispecific antibody conjugated to the CD displays a low affinity to transferrin receptors (TfRs) which allows the probe to cross the blood-brain barrier via receptor mediated transcytosis leading to a minimally invasive diagnosis. A synthesis technique was developed to conjugate the bispecific antibody to the CD. As a proof of concept, this technique was used to couple bovine serum albumin (BSA) to CDs. The structural and optical properties of the CDs were observed. By synthesizing a novel carbon dot conjugated specific antibody that emits light at a specific wavelength in the near-infrared region, the molecular probe displays optical properties suitable for the minimally-invasive diagnosis using fNIR-spectroscopy.

Introduction: Alzheimer's disease is the most common form of dementia and is the 5th leading cause of death in the world. Alzheimer's disease is a chronic, neurodegenerative disease where the death of brain cells causes memory loss and cognitive decline, which usually starts slowly and worsens over time. The two most commonly studied biomarkers of Alzheimer's disease are amyloid-beta ($A\beta$) and tau. $A\beta$ as a diagnostic and therapeutic target has been an area of intense research as current diagnostic tools focus on $A\beta$ plaques. However, the assemblies of these plaques occur at the end of the $A\beta$ cycle and do not act as a good biomarker for diagnosing the early-onset of Alzheimer's disease.¹ Consequently, early diagnosis and treatment options are currently unavailable.

Objective: Develop a minimally-invasive nanoparticle-bound antibody that could be used for the early diagnosis and treatment of Alzheimer's by crossing the blood-brain barrier (BBB) using receptor-mediated transcytosis and specifically target $A\beta$ oligomers.

Hypothesis: I hypothesized that developing a bispecific antibody, generated from an anti- $A\beta$ oligomer-specific antibody Fab' (fragment) and an anti-TfR antibody Fab', can be used as an effective diagnostic probe for Alzheimer's disease. The bispecific antibody will have a low affinity to transferrin receptors which will allow it to cross the blood-brain barrier using receptor-mediated transcytosis. Furthermore, I hypothesized that due to the anti- $A\beta$ oligomer-specific antibody Fab, the bispecific antibody will have a high affinity to $A\beta$ oligomers and not have cross reactivity with $A\beta$ plaques and monomers. I hypothesized that by conjugating carbon dots (CDs) to bispecific antibodies (BsAbs), the molecular probe could emit light in the near infrared region which can be detected using fNIR-spectroscopy. The probe allows for a minimally invasive diagnosis of Alzheimer's disease.

Method: The aim of the project is to develop a minimally-invasive, nanoparticle-bound antibody molecular probe for the early detection of Alzheimer's disease. The synthesis process consists of 3 steps: 1. Synthesize bispecific antibody. 2. Conjugation of bispecific antibody to carbon dot. 3. Determine optical properties of the molecular probe.

Synthesis of Bispecific Antibody: Current diagnostic tools identify A β plaques in cerebrospinal fluid via a lumbar puncture. New research suggests that A β plaques are present at similar concentrations in healthy individuals making them ineffective biomarkers.² Moreover, A β oligomers are present during the earliest stages of the disease and are found in significantly higher concentrations in patients with Alzheimer's disease. The A β oligomers distribution and abundance in the brain suggest they are better predictors of disease progression, making them attractive biomarkers.³ The molecular probe will target A β oligomers by consisting partly of an anti-A β oligomer-specific antibody Fab'.

The BBB is a highly selective permeable barrier formed by capillary endothelial cells which prevents roughly 98% of all designed therapeutics from entering the brain.⁴ Current research suggests that antibodies with a low affinity to transferrin receptors (TfRs) can cross the blood-brain barrier via receptor mediated transcytosis.⁵ The anti-transferrin receptor antibody binds to transferrin receptors and is transported across the endothelial cell that form the BBB. The antibody is then released from the transferrin receptors and into the brain once it has completely crossed over due to the low affinity of the antibody.⁶ The molecular probe will cross the BBB by consisting partly of an an anti-TfR antibody Fab'.

Bispecific Antibodies are antibodies that can simultaneously bind two separate and unique antigens.⁷ The bispecific antibody being synthesized consists of fragments of an anti-A β oligomer-specific antibody and anti-TfR antibody. The anti-A β oligomer-specific antibody

and the anti-TfR antibody were bought from a supplier. The fragments were generated using 2-mercaptoethylamine (MEA) (**Fig.1A**). 2-mercaptoethylamine is a disulfide reducing agent which can cleave the disulfide bonds in an antibody. The process of synthesizing the bispecific antibody (**Fig.1B**).

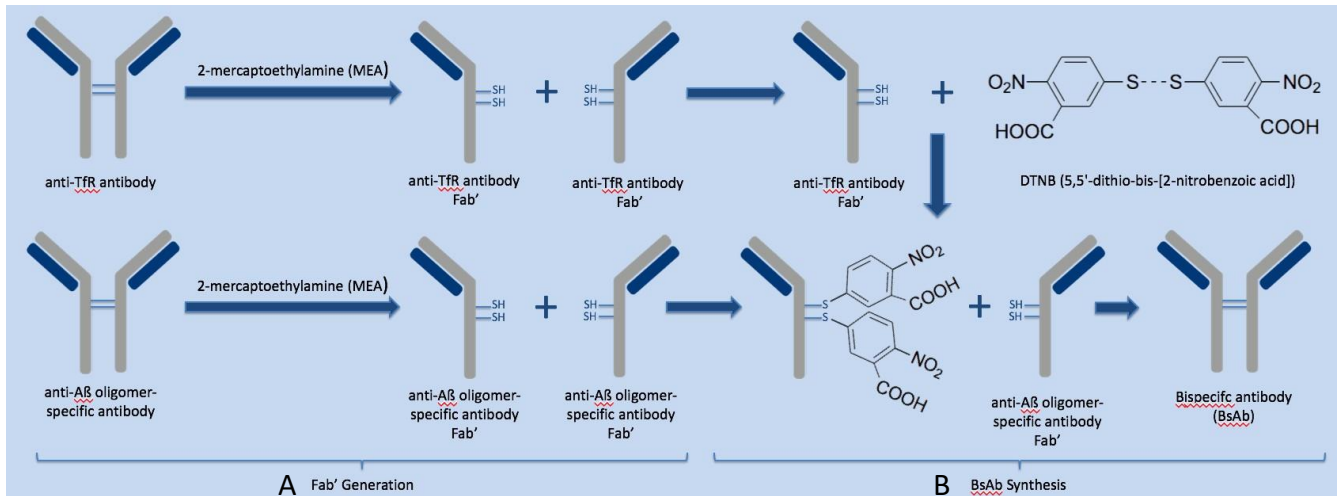


Figure 1: Generation of bispecific antibody from fragments of an anti-A β oligomer-specific antibody and anti-TfR antibody (A) Fab' generation. (B) BsAb synthesis.

Conjugation of Bispecific Antibody to Carbon Dot: Past research has explored the use of organic fluorophores and quantum dots which are prone to photo-bleaching, have less photo-stability, narrow excitation and emission wavelength (no possibility of tuning the optical properties) and cytotoxicity (organic fluorophore may change the metabolism of live cells during the bio-imaging process).⁸

Carbon Dots have drawn much attention due to their versatile physical, chemical and optical properties which make them superior to organic fluorophores and quantum dots as

they have higher fluorescence, improved photo stability, resistance to photo-bleaching and photo-blinking, facile surface functionalization and exhibit low cytotoxicity.⁹ They are amorphous with a sp^2 hybridized network of carbons.¹⁰ They can be prepared with a plethora of starting materials improving cost efficiency of the molecular probe.¹¹ Normally CDs are made to be hydrophilic but could be designed to also be hydrophobic and amphipathic.^{12,13} Due to the quantum confinement effect, the carbon dot can vary in optical properties (absorption, emission wavelengths and emission quantum yield) simply by changing the particle size during the synthesis process.¹⁴ Carbon dots are superior to quantum dots as they are significantly less toxic as during the bio-imaging process, quantum dots release toxic metals which leads to a change in metabolism in live cells.¹⁵ Carbon dots have tunable optical properties that span the UV to near infrared regions which make them suitable nanoparticles for fNIR spectroscopy.^{16,17}

The carbon dots can be effectively tuned for conjugation when compared to the tunable properties of a protein. The unconjugated CDs contain terminal amine groups which if not altered, can lead to inter-conjugation amongst the CDs. The carboxyl groups can be easily coupled to the unprotonated, NH_2 groups found on the bispecific antibody.¹⁸

The surface of the CDs plays a primordial role in dictating their optical and structural properties. The surface was evaluated using fourier-transform infrared spectroscopy (FTIR) (**Fig.2A**). The carboxylic acid $C=O$ stretching band at 1715 cm^{-1} was observed. This is accompanied by the concomitant appearance of amide $C=O$ and $C=C/C=N$ bending peaks at 1645 and 1550 cm^{-1} respectively. The absence of a primary amine stretch is typically observed between 3300 and 3500 cm^{-1} suggests that the primary amines reacted to form amides (**Fig.2B**).

It is noteworthy to mention that sp^3 C–H stretching bands at 3100 cm^{-1} and sp^2 C–H at 2875 cm^{-1} are observed because of the short carboxylic acid OH stretch. These peaks suggest there is a decreased amine content in comparison to carboxyl groups (**Fig.2C**).

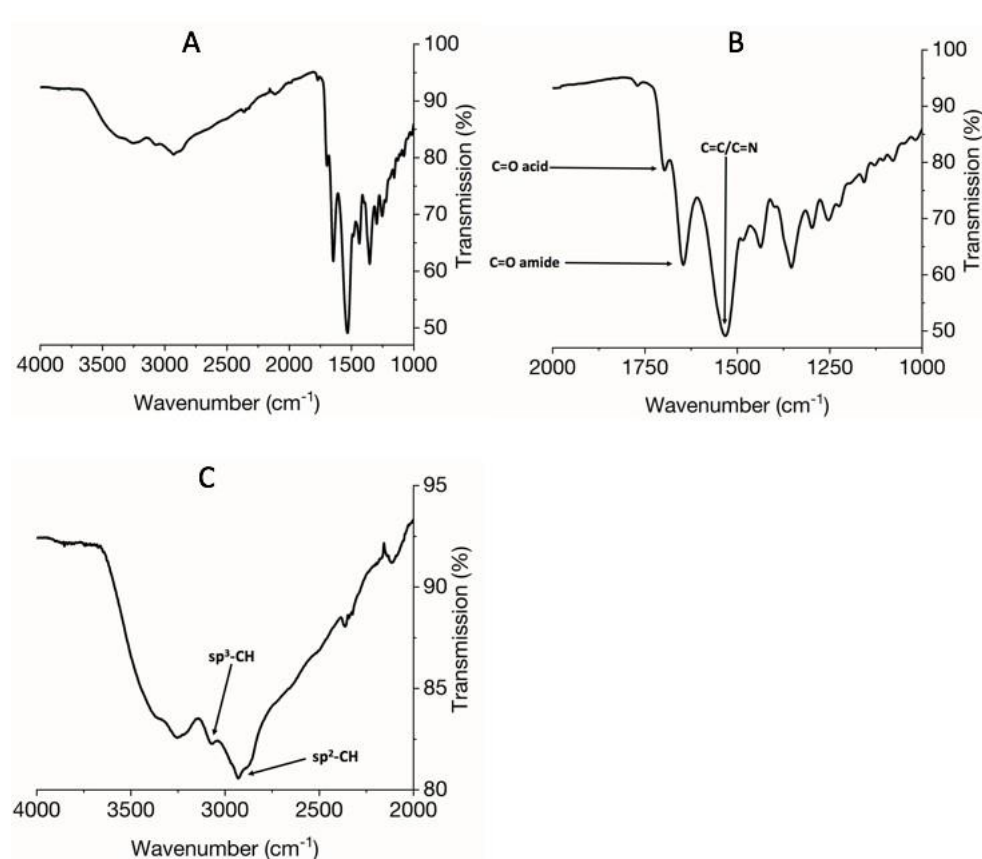


Figure 2: FTIR spectra of CDs (A) FTIR Spectra shown over spectral range of 1000 to 4000 cm^{-1} . (B) FTIR Spectra shown over spectral range of 1000 to 2000 cm^{-1} . The spectra reveal the presence of carboxylic and amidic carbonyl groups as well as C=C/C=N moieties on the surface of the CDs. (C) FTIR Spectra shown over spectral range of 2000 to 4000 cm^{-1} . The spectra reveal the presence of sp^2 and sp^3 C–H

As there is amine residue on the lysine's present in the amino acid sequence of the protein, it can act as the site of conjugation. Naturally, the reactive amine groups found on the

protein are protonated, NH_3 groups which can lead to inter-conjugation amongst the protein. By altering the pH of the solution mixed with the protein when preparing for conjugation, it can affect the pKa. By reaching a specific pH, all of the amine residue found on the lysine's of the protein can be unprotonated NH_2 groups which will prevent inter-conjugation and act as the site of conjugation to the CDs.

2,4,6-trinitrobenzene sulfonic acid (TNBS) modification was used for the quantification of primary amines present on the lysine's of the protein. The reaction of TNBS with primary amines produce a highly chromogenic product which can be readily measured at 335 nm using UV-Vis spectroscopy (**Fig.3A**).

As a proof of concept, bovine serum albumin (BSA) was used to be coupled with the CDs as it shares a similar amount of lysine's. CDs in MES buffer solutions of different pH's were prepared and tested with TNBS to determine which produced no reactive amine groups. A CD solution of 4.6 pH was found to have no free amine groups on surface which is optimal for conjugation with CDs.

Carbon dots contain carboxyl groups which can be covalently bonded to the amine group found on the bispecific antibody synthesized using 1,2-dichloroethane (EDC) and N-hydroxysulfosuccinimide (NHS) (**Fig. 3B**). The CD conjugated BSA can be filtered from the unconjugated CDs through a centricon tube. After centrifuging the centricon tube, the unconjugated CDs can be removed from the sample leaving only the CD-bound BSA. The 30 KDa molecular cut off washed out unbound CDs and BSA.

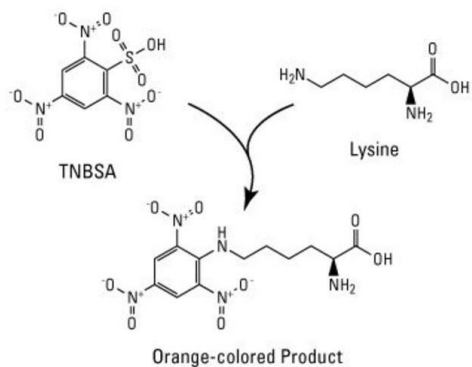
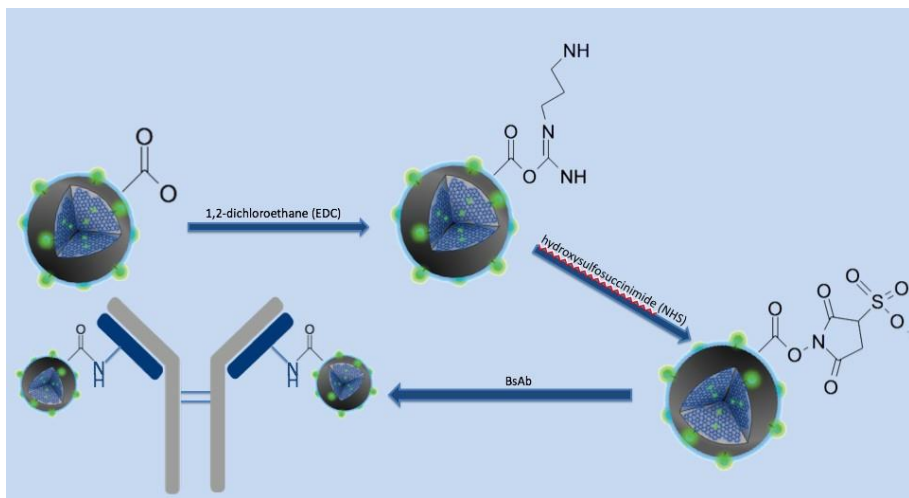
A**B**

Figure 3: (A) TNBS modification reaction used for the quantification of primary amines (B) BsAb and CD conjugation.

Coupling of CD and BSA was observed using denaturing agarose gel electrophoresis. The agarose gel was observed both stained with coomassie blue and Visualized under 365 nm light irradiation(**Fig.4**).

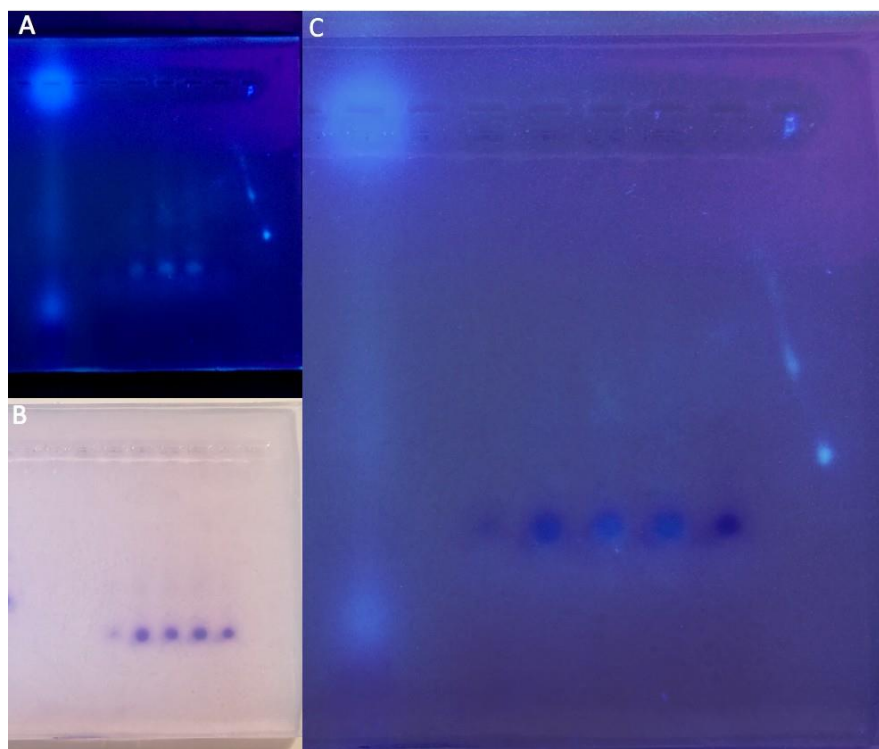


Figure 4: Images of CD bound BSA subjected to 4% denaturing agarose gel electrophoresis. The wells from left to right in each gel contain CD control, BSA control, CD bound BSA, CD bound BSA, CD bound BSA, BSA control. (A) Visualized under 365 nm light irradiation. (B) Agarose gel stained with coomassie blue. (C) Overlay of (A) and (B).

Determining the Optical Properties of the Molecular Probe: Light in the near infrared region (NIR) can be used for deep tissue imaging which allows for increased penetration and limited scattering of NIR light by biological tissue when compared to other regions including visible light. The visible (VIS) and near- infrared (NIR) wavelengths for in vivo imaging is between 450 and 1000 nm.²⁰ The exact origin of the fluorescence emission nature of carbon dots is an area of intense research as the reason remains debatable. The type of emission that will be observed with the molecular probe is the first class bandgap

transition caused by π -domains. The mechanism allows the carbon dots to display strong emission of UV-visible-NIR light, thus allowing the carbon dot to be detected using fNIR spectroscopy.²¹

Ultraviolet-visible (UV-Vis) spectroscopy was done to determine the optical properties of the CDs synthesized. The CDs exhibited a broad absorption spectrum from 275 to 425 nm, with transition bands at 241 and 354 nm (**Fig. 5A**). The first and second bands can be ascribed to the $\pi \rightarrow \pi^*$ and $n \rightarrow \pi^*$ transitions of the aromatic sp^2 domains for the C=O, as well as the C=S/C=N bonds, respectively. The contour plot indicates that the luminescence profile of the CDs are similar with an excitation λ_{\max} at ~ 350 nm and fluorescence λ_{\max} at ~ 450 nm (**Fig. 5B**). The CDs synthesized exhibit a quantum yield of 59.1% which result in a much greater fluorescence intensity in comparison to other manufactured CDs (**Fig. 5C**). The CDs have a molar extinction coefficient of 14500 mol^{-1} .

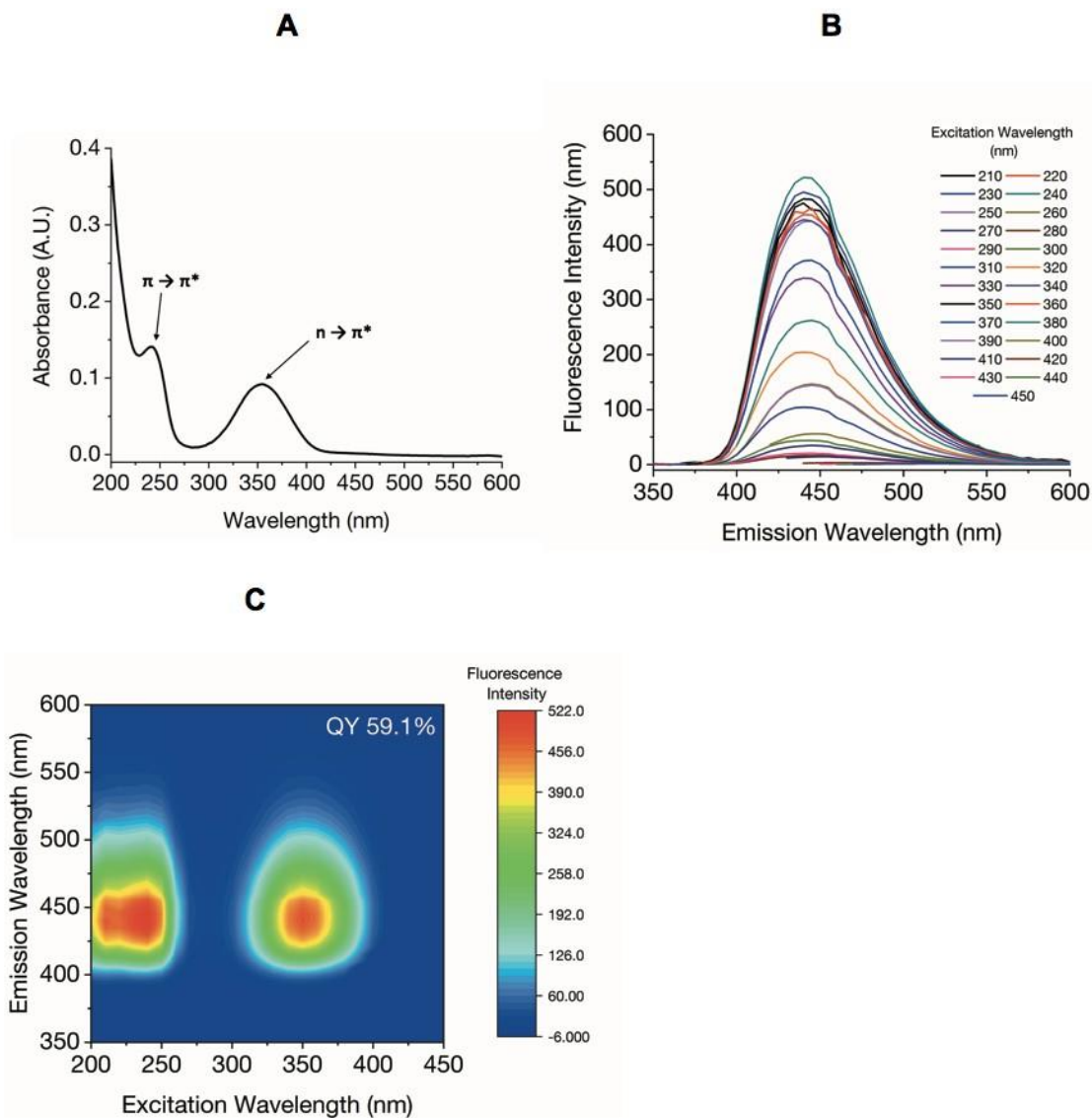


Figure 5: Optical properties of DT3-CD (5 $\mu\text{g/mL}$ in MilliQ water). (A) UV-Vis absorption spectra of DT3-CD. (B) fluorescence spectra of DT3-CD. (C) fluorescence contour plots of DT3-CD.

The carbon dot synthesized that will be used in developing the molecular probe emits light maximally around 450 nm and has a quantum yield of 59.1% which suggests it can be tuned to be between 700 nm-900nm, suitable for non-invasive fNIR spectroscopy. Have CDs

that can emit at such a high intensity at just 450 nm can be used for other types of spectroscopy in the brain. The carbon dots exhibit great extinction coefficients which leads to a more precise diagnosis. The CDs have a broad absorption spectrum of 275 to 425 nm, making them more practical due to a single excitation source being required as supposed to multiple. The carbon dots have a larger stoke shift as supposed to organic fluorophores and quantum dots which allow for the detection of fluorescence and reducing interference. The molecular probe would be significantly brighter in comparison to a quantum dot probe or organic fluorophore probe due to the high extinction coefficients (amount of light of specific wavelength absorbed by the CDs) and quantum yield.

The molecular probe has the potential for a therapeutic effect as it displays low cytotoxicity and decreases the amount of A β oligomers free floating in the brain preventing the build up of A β plaques. This will lead to increased cell life span by the molecular probe immobilizing the most toxic form of A β .

Conclusion: 50 million people worldwide are living with Alzheimer's disease with the number expected to reach 75 million by the year 2030. An early diagnosis is crucial to treat the disease, however, current methods detect Alzheimer's during the later stages, once the irreversible damage has been done. Thus, the aim of my project was to develop a minimally-invasive molecular probe that could be used for the early diagnosis of Alzheimer's.

By conjugating a carbon dot to BSA with a quantum yield of 59.1%, it sets up the downward workflow for the synthesis technique for the molecular probe designed.

By synthesizing a bispecific antibody conjugated to a carbon dot that emits light at a specific wavelength in the near-infra red region, the molecular probe displays optical properties suitable for the minimally-invasive diagnosis using fNIR-spectroscopy. The NIR can

penetrate brain tissue to a depth of up to 8 cm.²² This is roughly the radius of the average head worldwide. The molecular probe has the potential to cross the blood-brain barrier due to its low affinity to transferrin receptors, allowing it to cross using receptor-mediated transcytosis. The probe has a high affinity towards A β oligomers, allowing the concentration of this biomarker to be measured.

The concept behind the development of the minimally-invasive, nanoparticle-bound antibody could be implemented into an effective treatment and diagnostic tool for other neurodegenerative diseases. This research opens the door to other follow up experiments in determining a more efficient and effective diagnosis of Alzheimer's, which prevents late diagnosis and ultimately saves the lives of millions.

Advantages and Disadvantages:

They can be prepared plethora of starting materials improving cost efficiency of the molecular probe. This minimally-invasive design can be applied in a diagnostic and therapeutic manner. Current infrared carbon dots do not remain in an excited state for long periods of time. This is why near-infrared carbon dots with high quantum yields were synthesized first to create the downward workflow for the synthesis of infrared carbon dots.

Further Research:

I plan to test this novel design of a carbon dot-bound BsAb in vivo with a synthesized infrared emitting CD and perform cytotoxicity tests. Furthermore, I would like to build on the design and focus on its therapeutic effects. The design could be implemented for other diseases in the brain.

Materials and Methods:

Microwave synthesis of citric acid-based carbon dots

CDs were synthesized using a CEM Discover SP microwave reactor. Briefly, 0.384 g (500 mM) of citric acid was added to 4 mL of water in a glass microwave reaction tube.

Subsequently, the concentration of the passivating agent was varied from 125 to 750 mM.

The reaction mixture was allowed to heat to temperatures ranging from 180 to 220 °C for a period of 10 min. Upon reaction completion, the crude samples were dialyzed in Milli-Q water, using 1 kDa MWCO dialysis bags (Spectra/Pors6 RC – Spectrum Laboratories).

During this process, there is a visible and progressive decrease in the color and fluorescence of the dialysate. We further purify our material with 3 additional organic wash steps using acetone to further remove any impurities. Following dialysis, 40 mL of acetone was added to the dialyzed samples, vortexed for 30 seconds and centrifuged at room temperature at 10000 g for 10 min. The supernatant was discarded, and the organic wash procedure was repeated 2 additional times. With every purification step, we notice a progressive decrease in the fluorescence of the supernatant. Following the third organic wash, the supernatant is completely devoid of fluorescence, thus indicating that all impurities and unreacted materials have been removed. The resulting precipitate was dried overnight in an oven at 80 °C and was then crushed into a fine powder followed by dispersion in Milli-Q water.

Fourier-transform infrared spectroscopy (FTIR)

FTIR spectra were collected on the dried solid powder of CDs using a Thermo Scientific Nicolet iS5 equipped with iD5 ATR accessory. Analysis was performed on a laminate-diamond crystal window using 64 scans at 0.4 cm⁻¹ resolution.

Fluorescence spectra

Fluorescence spectra of aqueous CD dispersions were recorded using a Cary Eclipse Fluorescence Spectrophotometer from Agilent Technologies. To minimize the potential for inner filter effects, the concentration of the CDs, in water, was adjusted to an absorbance

value of 0.1 a.u. prior to analysis. Fluorescence spectra were recorded in a 1 cm quartz cuvette, using a λ_{ex} of 250–700 nm (varied in 10 nm increments for contour maps and 50 nm intervals). The excitation and emission slit widths were set to 2.5 and 5 nm, respectively, with a PMT voltage of 600 V. All data processing and all contour plots were generated using the Agilent Cary Eclipse application software.

Quantum yield determination

Quantum yield values were determined using a FLS920 Fluorescence Spectrometer (Edinburgh Instruments) equipped with an integrating sphere, using a 1 cm path length quartz cuvette. Both excitation and emission slit widths were set to 5 nm. λ_{ex} was set to 350 nm and the fluorescence spectrum was acquired from 300 to 800 nm. Triplicate scans were acquired with a dwell time of 0.2 s. The data were processed using the F900 software supplied by the manufacturer.

Preparation of carbon dots for conjugation

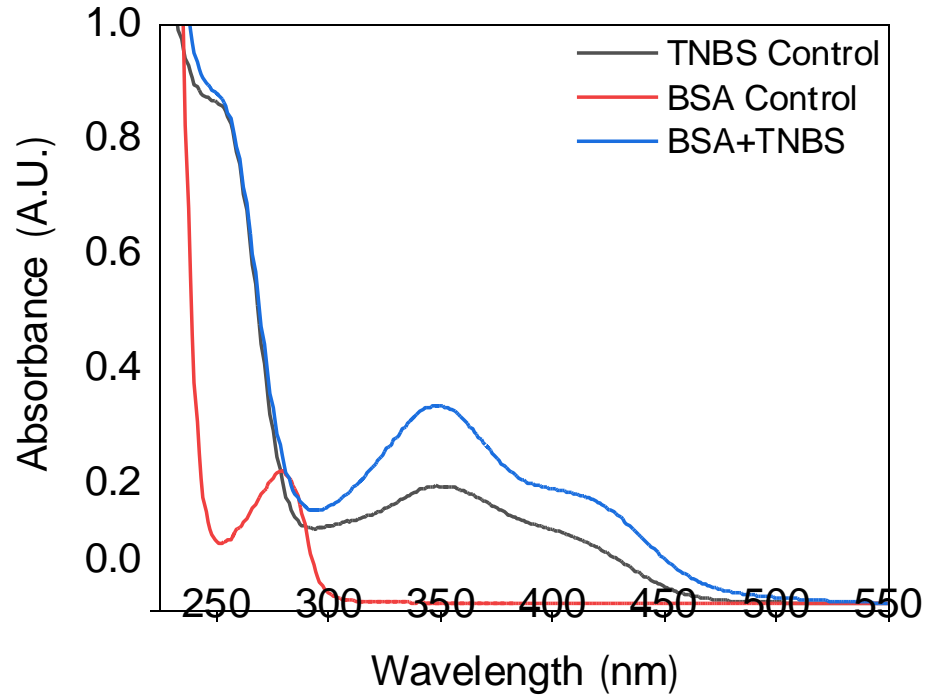
1.4 mg of Carbon dots was prepared in a 1.4mL solution of MES (buffer) at pH 4.6. 0.47935g of EDC was prepared in 5 mL of MES to create a 30mM solution. 0.014385g of NHS was prepared in 5 mL of MES for a 25mM solution. 200uL of EDC (30mM) and 200uL of NHS (25mM) was added to 1 mL of 1 mg/mL pH 4.6 carbon dots and stirred for 30 minutes. This activated the carboxyl groups on the CDs which can be covalently bonded to the amine group found on the BSA.

Conjugation of carbon dots to BSA

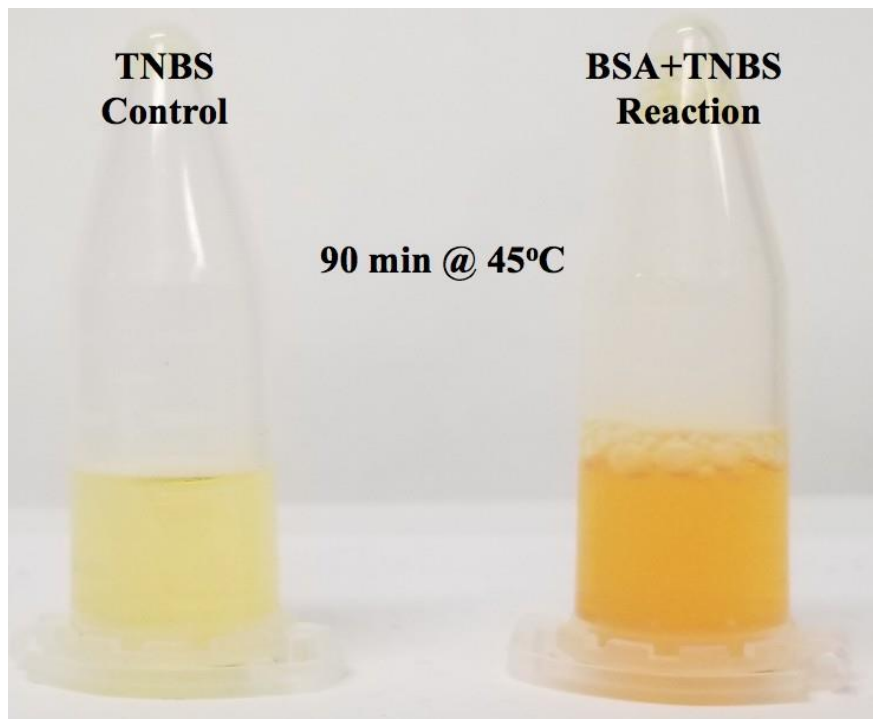
5 mL of the BSA solution (pH 7.5) was added to the CD, NHS, EDC solution and stirred for 1 hour and 30 minutes. A dialysis membrane prior to concentration was conditioned with 0.1 M potassium bicarbonate. MES buffer was added to the the BSA, CD, NHS, EDC solution in centricon tube and centrifuged at 5000 G up to 6 minutes several times until completely filtered. All unconjugated CDs were removed from centricon tube leaving only conjugated CD-BSA at the top. The centricon tube was stored in ethanol to preserve dialysis membrane.

Determination of reactive/accessible amines on the CDs

- **0.1M MES 0.9% NaCl pH 4.6**
 - 20 ug CDs @ 345nm = 0.340 A.U.
 - 10 uL TNBS in 5mLs 0.1M MES 0.9% NaCl pH 4.6 (control) = 0.853 A.U. @ 345nm
 - TNBS + CDs (1.5 hrs reaction in dark at 45°C = 1.191 A.U.
 - $0.34 + 0.853 = 1.193 \text{ A.U.} - 1.191 \text{ A.U.} \sim 0$
 - **NO reactive amines of the 500DT3-CDs at pH 4.6**
- **0.1M MES pH 6.0**
 - 20 ug CDs @ 345nm = 0.353 A.U.
 - 10 uL TNBS in 5mLs 0.1M MES pH 6.0 (control) = A.U. 0.823@ 345nm
 - TNBS + CDs (1.5 hrs reaction in dark at 45°C = 1.20A.U.
 - $0.353 + 0.823 = 1.176 \text{ A}$
 - $1.20 - 1.176 = 0.024 \text{ A.U.} = 1.7 \text{ uM}$
 - **0.083 uM reactive amines per ug of 500DT3-CDs at pH 6.0**
- **10 mM Potassium Phosphate pH 7.5**
 - 20 ug CDs @ 345nm = 0.351 A.U.
 - 10 uL TNBS in 5mLs 10 mM Potassium Phosphate pH 7.5 (control) = 0.835 A.U. @ 345nm
 - TNBS + CDs (1.5 hrs reaction in dark at 45°C (1/10) = 0.158A.U. (stock 1.58 A.U.)
 - $0.351 + 0.835 = 1.186 \text{ A.U.}$
 - $1.58 - 1.186 = 0.394 \text{ A.U.} = 27.2 \text{ uM}$
 - **1.4 uM reactive amines per ug of 500DT3-CDs at pH 7.5**



TNBS Reaction with BSA



Bibliography:

1. University of Texas Medical Branch at Galveston. (2018, August 17). Why some people with brain markers of Alzheimer's have no dementia. *ScienceDaily*. Retrieved March 22, 2019 from www.sciencedaily.com/releases/2018/08/180817093810.htm
2. Zolochovska, O., Bjorklund, N., Woltjer, R., & Wiktorowicz, J. E. (2012). Postsynaptic Proteome of Non-Demented Individuals with Alzheimer's Disease Neuropathology. *Journal of Alzheimer's Disease & Parkinsonism*, 02(04). doi:10.4172/2161-0460.1000e121
3. Wang-Dietrich, L., Funke, S. A., Kühbach, K., Wang, K., Besmehn, A., Willbold, S., . . . Willbold, D. (2013). The amyloid- β oligomer count in cerebrospinal fluid is a biomarker for Alzheimer's disease. Retrieved from <https://www.ncbi.nlm.nih.gov/pubmed/23313925>
4. Pardridge, W. M. (2005, January). The blood-brain barrier: Bottleneck in brain drug development. Retrieved from <https://www.ncbi.nlm.nih.gov/pmc/articles/PMC539316/>
5. Xiao, Liang-Shang, & Gan. (2013, June 11). Receptor-Mediated Endocytosis and Brain Delivery of Therapeutic Biologics. Retrieved from <https://www.hindawi.com/journals/ijcb/2013/703545/>
6. Yu, Y. J., Zhang, Y., Kenrick, M., Hoyte, K., Luk, W., Lu, Y., . . . Dennis, M. S. (2011, May 25). Boosting brain uptake of a therapeutic antibody by reducing its affinity for a transcytosis target. Retrieved from <https://www.ncbi.nlm.nih.gov/pubmed/21613623>
7. Hudson, P. J., & Souriau, C. (2003, January 01). Engineered antibodies. Retrieved from <https://www.nature.com/articles/nm0103-129>
8. Feng, L., Long, H., Liu, R., Sun, D., Liu, C., Long, L., . . . Xiao, B. (2013). A Quantum Dot Probe Conjugated with A β Antibody for Molecular Imaging of Alzheimer's Disease in a Mouse Model. *Cellular and Molecular Neurobiology*, 33(6), 759-765. doi:10.1007/s10571-013-9943-6
9. Luo, P. G., Sushant Sahu, S. Y., Sonkar, S. K., Wang, J., Wang, H., LeCroy, G. E., & Li Cao, Y. S. (2013, February 20). Carbon "quantum" dots for optical bioimaging. Retrieved from <https://pubs.rsc.org/en/content/articlelanding/2013/tb/c3tb00018d/unauth#!divAbstract>
10. Georgakilas, V., Perman, J. A., Tucek, J., & Zboril, R. (2015, June 10). Broad family of carbon nanoallotropes: Classification, chemistry, and applications of fullerenes, carbon dots, nanotubes, graphene, nanodiamonds, and combined superstructures. Retrieved from <https://www.ncbi.nlm.nih.gov/pubmed/26012488>
11. Katerina, Zhang, Yu, Wang, Yu, Giannelis, . . . L., A. (2014, October 01). Carbon dots- Emerging light emitters for bioimaging, cancer therapy and optoelectronics. Retrieved from <https://repository.kaust.edu.sa/handle/10754/597729>
12. Zhu, H., Wang, X., Li, Y., Wang, Z., Yang, F., & Yang, X. (2009, July 16). Microwave synthesis of fluorescent carbon nanoparticles with electrochemiluminescence properties. Retrieved from <https://pubs.rsc.org/en/content/articlelanding/2009/cc/b907612c#!divAbstract>
13. Xu, Z., Wang, C., Jiang, K., Lin, H., Huang, Y., & Zhang, C. (2015, November 04). Microwave-Assisted Rapid Synthesis of Amphibious Yellow Fluorescent Carbon Dots as a Colorimetric Nanosensor for Cr(VI). Retrieved from <https://onlinelibrary.wiley.com/doi/full/10.1002/ppsc.201500172#references-section>
14. Sun, Y., Zhou, B., & Lin, Y. (n.d.). Quantum-Sized Carbon Dots for Bright and Colorful Photoluminescence. Retrieved from <https://pubs.acs.org/doi/abs/10.1021/ja062677d>
15. Yang, S., Wang, X., & Wang, H. (n.d.). Carbon Dots as Nontoxic and High-Performance Fluorescence Imaging Agents. Retrieved from <https://pubs.acs.org/doi/abs/10.1021/jp9085969>

16. Martinic, I., Eliseeva, S. V., & Petoud, S. (2016, October 01). Near-infrared emitting probes for biological imaging: Organic fluorophores, quantum dots, fluorescent proteins, lanthanide(III) complexes and nanomaterials. Retrieved from <https://www.sciencedirect.com/science/article/pii/S0022231316308766>
17. Jhonsi, M. A. (2018). Carbon Quantum Dots for Bioimaging. *State of the Art in Nano-bioimaging*. doi:10.5772/intechopen.72723
18. Hang, B., & Wang, W. (2012, May 23). Polyethyleneimine modified fluorescent carbon dots and their application in cell labeling. Retrieved from <https://www.sciencedirect.com/science/article/pii/S0927776512002925>
19. Ranger, M., Johnston, C. C., Catherine Limperopoulos, C., Rennick, J. E., & Plessis, A. J. (2011, September/October). Cerebral near-infrared spectroscopy as a measure of nociceptive evoked activity in critically ill infants. Retrieved from <https://www.ncbi.nlm.nih.gov/pmc/articles/PMC3206783/>
20. Kim, H. Y., Seo, K., Jeon, H. J., Lee, U., & Lee, H. (2017, August 31). Application of Functional Near-Infrared Spectroscopy to the Study of Brain Function in Humans and Animal Models. Retrieved from <https://www.ncbi.nlm.nih.gov/pmc/articles/PMC5582298/>
21. Liu, Y. (2012, September 25). Synthesis of highly luminescent graphitized carbon dots and the application in the Hg²⁺ detection. Retrieved from <https://www.sciencedirect.com/science/article/pii/S0169433212016182>
22. Sultan, E., Manseta, K., Khwaja, A., Najafizadeh, L., Gandjbakhche, A., Pourrezaei, K., & Daryoush, A. S. (2011, February 11). Modeling and tissue parameter extraction challenges for free space broadband fNIR brain imaging systems. Retrieved from <https://www.spiedigitallibrary.org/conference-proceedings-of-spie/7902/790223/Modeling-and-tissue-parameter-extraction-challenges-for-free-space-broadband/10.1117/12.875618.short?SSO=1>
23. Hermanson, G. T. (2013). Introduction to Bioconjugation. *Bioconjugate Techniques*, 1-125. doi:10.1016/b978-0-12-382239-0.00001-7

【評語】 090027

Solid data and clear presentation. Very practical experimental design with great clinical application. We appreciate the clever combination of monoclonal antibody, carbon-nano technique, and AD biology. It's an outstanding project.